CORROSION SCIENCE AND TECHNOLOGY, Vol.24, No.6(2025), pp.444~452 pISSN 1598-6462 / eISSN 2288-6524
[Research Paper] DOI: https://doi.org/10.14773/cst.2025.24.6.444

Cathodic Protection Performance of ICCP System applied to Floating Offshore Reinforced Concrete Structure

Du-Hyeong Lee and Jin-A Jeong†

Division of Marine System Engineering, Korea Maritime & Ocean University, 727 Taejong-ro, Yeongdo-Gu, Busan 49112, Korea
(Received December 10, 2025; Revised December 13, 2025; Accepted December 15, 2025)

Reinforced concrete structures in marine environments frequently experience premature deterioration due to corrosion, particularly of the steel reinforcement, which is a leading cause of degradation in these structures, including bridges and marine airports. In recent years, developed countries have increasingly turned to offshore spaces—such as floating wind farms, floating solar power plants, and floating waste treatment facilities—for infrastructure development, driven by a shortage of available urban land. This trend is also observable in our country, where, despite being surrounded by the sea on three sides, usable land in urban centers is extremely limited. To mitigate corrosion in reinforced concrete structures, various cathodic protection methods are employed, including sacrificial anode cathodic protection (SACP) and impressed current cathodic protection (ICCP). Among these, ICCP is the preferred method due to the high electrical resistivity of concrete. In this study, we applied an ICCP system powered by self-generated energy sources—such as wind power, solar power, and ocean thermal energy—to floating reinforced concrete offshore structures. The performance of the ICCP system was assessed by measuring the cathodic protection current, cathodic protection potential, and depolarization potential.

Keywords: *Corrosion, ICCP System, SACP System, Potential, Resistivity*

1. Introduction

All around the world, industries rooted in the fossil fuel era are rapidly transitioning toward clean energy–based industries to achieve carbon neutrality, and nations are competing to take the lead in related technologies [1]. Considering the geographical characteristics of South Korea—where three sides are surrounded by the sea but available land in urban centers is extremely limited—it is essential to utilize maritime space for urban development and social infrastructure.

In shipbuilding and marine-related fields, including ships, port facilities, bridges, transmission towers, subsea pipelines, offshore wind power facilities, airports, and offshore plants, concerns regarding the reduction of residual service life due to the corrosive marine environment are inevitable [2-4]. In particular, rapid industrialization driven by economic development in developing countries has led to a significant increase in waste generation. Under current conditions, where environmental issues such as global warming are of major concern, the treatment of industrial waste has emerged as a serious social problem [5]. South Korea is no exception and is therefore seeking alternative sites due to restrictions on the use of metropolitan landfill areas. Several advanced countries have imposed strict environmental regulations on waste treatment and are addressing these challenges by constructing offshore waste treatment facilities equipped with eco-friendly technologies, thereby establishing systems to transport and process land-generated waste via marine routes. For example, Japan is constructing ultra-large floating offshore waste treatment facilities off the coasts of Tokyo and Osaka, and the number of such floating offshore structures is increasing. In advanced countries such as the Netherlands, where much of the land lies below sea level, as well as coastal nations including Denmark and Singapore, and island nations such as the United Kingdom and Japan, floating offshore structures have already been implemented [6]. These structures contribute to resource conservation through renewable energy generation, such as solar power, and, because they are floating, they are less vulnerable to flooding disasters caused by sea-level rise.

†Corresponding author: jina@kmou.ac.kr
Du-Hyeong Lee: Associate Professor, Jin-A Jeong: Professor

Globally, land resources are limited, while population growth and natural disasters induced by global warming—such as glacier melting and rising sea levels—are causing widespread damage. In this context, floating offshore structures integrated with renewable energy systems are attracting considerable attention as potential solutions to these challenges.

Recently, increasing attention has also been focused on eco-friendly energy technologies, including floating offshore wind power and floating solar power projects [7]. Since coastal waters near urban centers must be developed in an environmentally sustainable manner and serve as eco-friendly spaces for citizens, indiscriminate land reclamation or environmentally destructive construction of energy infrastructure is no longer acceptable. Consequently, extensive research on floating offshore structure technologies is being conducted worldwide. These technologies offer the potential for widespread application along the national coastline in the future. However, as these structures are installed in marine environments, corrosion caused by seawater is unavoidable, and appropriate protection methods must be implemented to ensure their design service life. Although the literature presenting concrete field-based case studies on the application of ICCP to floating reinforced concrete offshore structures remains limited, performance evaluation studies of ICCP systems applied to existing marine concrete structures—such as offshore bridge substructures and marine pier facilities—suggest that their applicability can be extended to floating structures. Furthermore, ICCP design guidelines and practical engineering documents classify submerged and seawater-exposed zones of floating structures as structural components suitable for ICCP application, and provide design principles for system selection as well as for current distribution and control. Therefore, systematic studies on the applicability and protection performance of ICCP systems for various types of floating offshore structures are considered essential for future development.

To mitigate corrosion in marine structures, cathodic protection methods such as sacrificial anode cathodic protection (SACP) systems using aluminum or zinc and impressed current cathodic protection (ICCP) systems employing a direct current power supply and insoluble anodes can be applied [8,9].

Floating offshore plant facilities constructed with reinforced concrete can utilize self-generated electricity from renewable sources such as solar and wind power, enabling eco-friendly cathodic protection. However, the cathodic protection behavior of such floating facilities has not yet been sufficiently investigated. Although ICCP systems are effective in high-resistivity environments, their performance may vary depending on exposure conditions, leading to issues such as overprotection, underprotection, and electrical short circuits.

To differentiate this study from previous research on the application of ICCP to reinforced concrete, a large-scale reinforced concrete mock-up specimen was installed in an actual marine mooring environment. Its cathodic protection characteristics were investigated to evaluate the applicability of ICCP systems to floating offshore plant facilities. An ICCP system capable of supplying protection current in a semi-permanent manner was applied to a floating reinforced concrete offshore structure. The cathodic protection current, cathodic protection potential, and depolarization potential were measured to assess the performance of the impressed current cathodic protection system.

2. Experimental method

2.1 Corrosion potential measurement

The corrosion potential indicates the thermodynamic tendency of reinforcing steel embedded in concrete to undergo corrosion under natural conditions. A silver/silver chloride (Ag/AgCl) reference electrode was used for potential measurements. The corrosion potential of the reinforcing steel was determined by placing the concrete electrolyte between the terminal connected to the rebar and the Ag/AgCl reference electrode, and measuring the potential difference between the two electrodes using a high-impedance multimeter. To minimize errors caused by the IR drop associated with the concrete's electrical resistance, the Ag/AgCl reference electrode was embedded within the specimen. The measured corrosion potential values were evaluated to determine the probability of corrosion in accordance with ASTM C876 specifications [10].

2.2 Concrete resistivity measurement

Concrete resistivity has a significant influence on the flow of corrosion current and therefore serves as a critical parameter for diagnosing whether reinforced concrete is

exposed to a corrosive environment. The initiation and propagation rates of rebar corrosion vary depending on the properties of the cement and the permeability of the concrete. Because the electrical conductivity of concrete reflects the ease of ionic migration through the pore solution, highly permeable concrete exhibits higher conductivity and, consequently, lower resistivity. Accordingly, measuring concrete resistivity allows the probability of corrosion of reinforcing steel embedded in concrete to be indirectly assessed.

For resistivity measurement, sensors may employ four small metal pins, or alternatively, two pins may be used to monitor relative changes in concrete resistance (impedance) over time rather than absolute resistivity. In this study, concrete resistance was measured using two probes installed at fixed intervals in a monitoring sensor, employing a Nilsson soil resistivity meter in accordance with ASTM G57 [11].

2.3 Depolarization potential measurement

To verify the adequacy of cathodic protection applied to reinforced concrete, the polarization potential was evaluated by monitoring depolarization after interrupting the power supply to the cathodic protection system. The 100 mV depolarization (100 mV decay) criterion, established by the National Association of Corrosion Engineers (NACE) and widely accepted internationally, defines effective cathodic protection as achieving a cathodic polarization of at least 100 mV on the protected steel reinforcement [12]. In this context, the cathodic polarization potential refers to the net polarization potential, excluding potential variations caused by the IR drop associated with concrete resistance or external environmental resistance.

When the cathodic protection current is applied and subsequently interrupted, the measured potential increases instantaneously. Within the first 5 seconds after power interruption, a sharp potential jump is observed, followed by a gradual increase until the equilibrium potential is reached. The initial sharp rise corresponds to the IR drop resulting from the electrical resistance of the concrete, whereas the subsequent gradual change reflects the cathodic polarization induced by the applied current. The depolarization portion represents the recovery of the steel surface toward its original natural corrosion state.

2.4 Mock-up specimen

A mock-up specimen was fabricated with dimensions of 300 cm × 500 cm × 250 cm, and both the bottom slab and wall thicknesses were set to 25 cm. The materials and mix proportions used for the concrete are listed in Table 1. The maximum size of coarse aggregate was limited to 25 mm, considering the spacing of the reinforcing bars within the specimen. After placement in the formwork, the concrete was cured in air for 30 days.

Deformed reinforcing bars (D16) were used and secured with wire to ensure electrical continuity. For potential measurements, screws were installed in two reinforcing bars to connect electrical wires, which were then routed to the terminal box of the power supply panel located onshore.

Fig. 1 through 3 illustrate the design and fabrication process of the mock-up specimen. After curing and removal of the formwork, the cathodic protection system was installed. On the right-hand side surface of the specimen, 20 mm-wide slots were machined horizontally at 260 mm intervals (eight rows) and vertically at 1,370 mm intervals (three rows). Titanium ribbon anodes were embedded in the horizontal slots, and to ensure uniform current distribution, the Ti ribbon anodes in the vertical slots were electrically connected to a stainless steel conductor bar by spot welding. A feeder wire was then connected to the top of the conductor bar on the far-right side to supply the protection current, with the wire end connected to the terminal box of the onshore power supply panel. The reference electrodes and sensors were installed at two locations at the center of the specimen, at heights of 100 cm (submerged zone) and 200 cm (atmospheric

Table 1. Concrete mixed design of the mock-up specimen

Gmax (mm)	Slump (mm)	Air (%)	W/C (%)	Admixture (kg)	Water (kg)	Cement (kg)	S (kg)	Ga (kg)
25	150	4.5	45.6	141	161	212	871	951

Gmax : maximum aggregate size, Ga : coarse aggregate, S : fine aggregate

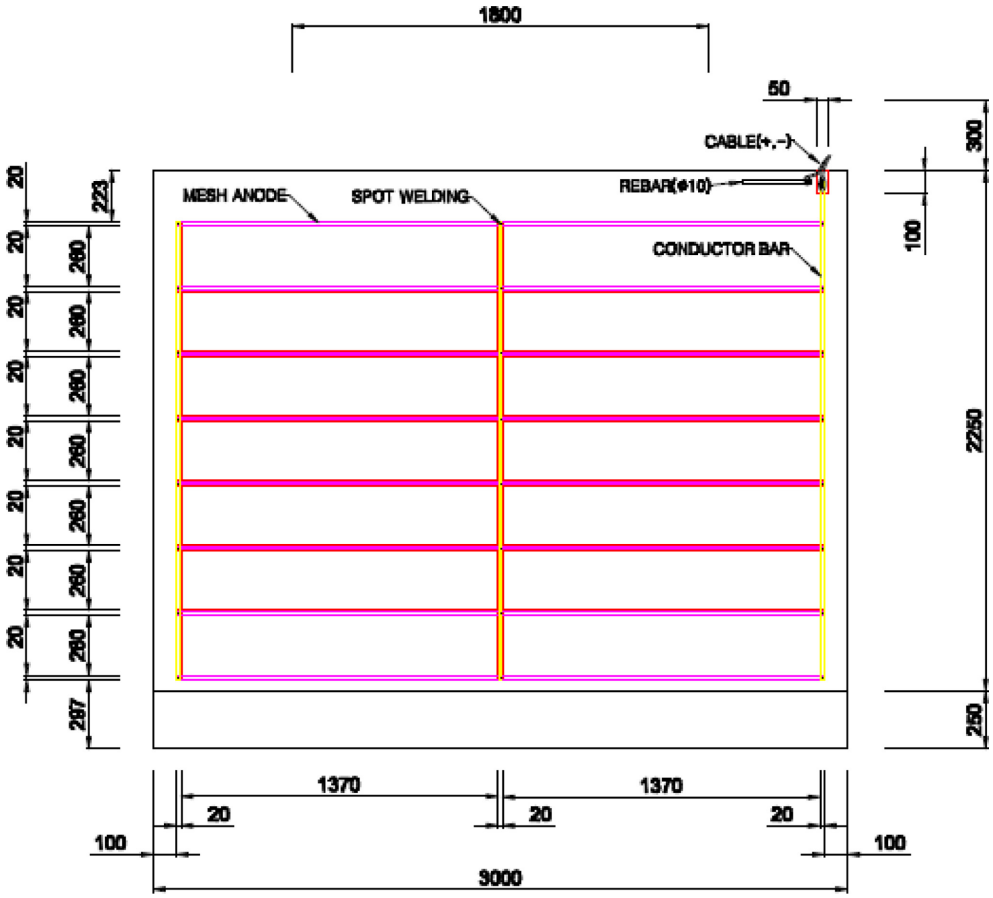

Fig. 1. Cross-sectional design of mock-up specimen and arrangement of Ti ribbon anode

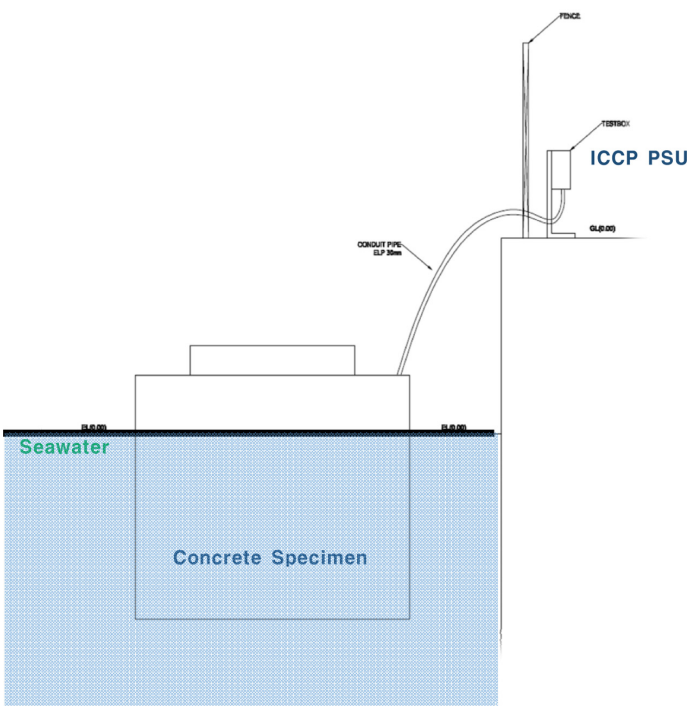

Fig. 2. Schematic drawing of floating mock-up specimen with ICCP power supply unit

(a) (b) (c)

Fig. 3. Appearance of the reference electrode (a) and monitoring sensor (b) fixed to the placed rebar and electrical connection part (c) of the rebar and the negative pole of the power supply unit

Fig. 4. Location of experimental mock-up specimen at harbor of KMOU

zone) measured from the bottom of the specimen. The reference electrode located in the submerged zone was used for monitoring the ICCP potential.

The specimen was installed at the training ship pier of Korea Maritime & Ocean University, as shown in Fig. 4. It was submerged to a depth of 170 cm in seawater, while the upper 80 cm remained above the sea surface and was exposed to the atmosphere, as illustrated in Fig. 2.

For specimens exposed to seawater, the corrosion potential, cathodic protection potential, depolarization potential, and concrete resistance were measured. The corrosion potential, cathodic protection potential, and depolarization potential were determined using reference electrodes embedded at locations within the submerged zone and the atmospheric zone above the seawater surface, as shown in Fig. 4a.

3. Experimental results

The corrosion potentials were measured after the mock-up specimen was floated in seawater. The corrosion potentials in the atmospheric and submerged zones were

(a) (b)

Fig. 5. The appearance of the mock-up specimen with slots for installing anodes machined on the surface after removing the formwork (a) and the ribbon anode installed in the slot and electrically connected to the stainless steel conductor bar by spot welding (b)

approximately −308 mV/SSCE and −317 mV/SSCE, respectively, indicating relatively low potentials. In the submerged zone, moisture was presumed to have already reached the reinforcing steel due to prolonged immersion, resulting in ongoing corrosion. In the atmospheric zone, the reference electrode was positioned close to the seawater level; therefore, seawater absorbed into the concrete likely contributed to the reduced corrosion potential. Nevertheless, the corrosion potential of the reinforcement in the atmospheric zone was slightly higher than that in the submerged zone. This difference can be attributed to variations in moisture content, chloride penetration, and concrete resistivity.

Pangrazzi reported that, in concrete pile specimens, chloride concentration varied with vertical height due to capillary action of seawater driven by tidal fluctuations [13]. Based on these findings, it is inferred that the submerged zone, which experienced greater seawater absorption and higher chloride content, exhibited more severe reinforcement corrosion and lower potentials, whereas the atmospheric zone, with relatively lower seawater and chloride ingress, showed slightly higher corrosion potentials.

Fig. 6 illustrates the variation in cathodic protection (CP) current and CP potential of the mock-up specimen over 270 h of CP application. An impressed current cathodic protection (ICCP) system was employed, with the CP potential controlled at −1000 mV/SSCE. Initially, a high CP current of approximately 90 mA was supplied; however, within a few minutes, it decreased to below 10 mA and subsequently stabilized. Upon application of cathodic protection, the CP potentials at all measured heights rapidly shifted in the negative direction due to current supply through the Ti ribbon anodes and then stabilized at constant levels.

The CP potential was evaluated based on the reference electrode installed in the submerged zone, following conventional practice. This approach was adopted because the specimen had been exposed to seawater for an extended period prior to CP application, allowing seawater to penetrate the concrete and reduce resistivity even in regions above the waterline. As a result, similar CP potentials were observed at different heights. Furthermore, increased moisture content in the concrete enhanced cathodic polarization under the applied CP current, leading to further reductions in CP potential. These results confirm that cathodic protection was effective not only in the submerged zone but also in regions near the seawater surface.

Fig. 7 shows the concrete resistance measured by sensors installed in the submerged and atmospheric zones. In the submerged zone, resistance was low from the beginning of the experiment, approximately 1.5 kΩ, and gradually decreased to about 0.9 kΩ after 270 h. In contrast, the atmospheric zone initially exhibited a high resistance of 13.2 kΩ, which decreased over time to approximately

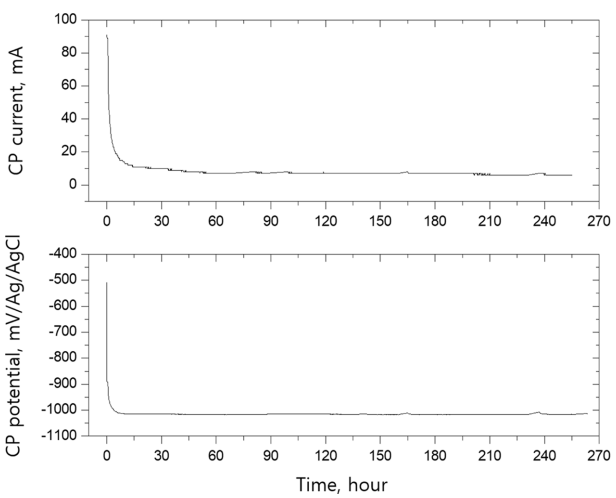

Fig. 6. Variation of cathodic protection current from the power supply unit to the rebar (upper) and cathodic protection potential measured with Ag/AgCl reference electrode (lower) with time

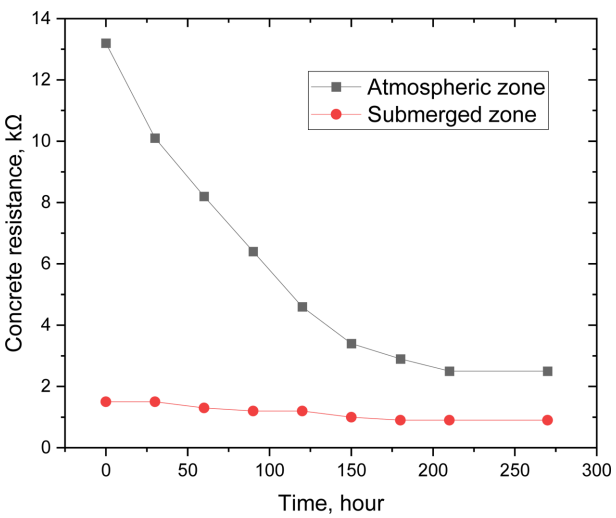

Fig. 7. Variations of concrete resistance measured from 2-probe sensor at upper part and lower part of the mock-up specimen with time

2.5 kΩ after 270 h. This behavior reflects continuous seawater exposure in the submerged zone, resulting in persistently low resistance, whereas the atmospheric zone initially remained dry and gradually absorbed seawater, leading to a progressive decrease in resistance.

According to the two-electrode corrosion assessment criterion, concrete environments with resistivity below 10 kΩ are considered highly corrosive and to provide little corrosion prevention capability. Based solely on resistivity, the range of 1 ~ 2 kΩ observed under seawater exposure in this study indicates that the reinforced concrete was subjected to a highly corrosive environment. However, with the application of an ICCP system, such low-resistivity conditions are advantageous, as they facilitate efficient current delivery from the anode to the reinforcing steel, thereby enhancing corrosion protection performance.

The measured resistivity in the submerged zone ranged from 0.9 to 1.5 kΩ, reflecting variations in moisture content. As reported by Presuel-Moreno et al., unlike permanently submerged regions, atmospheric zones exhibit reduced depolarization due to higher resistivity associated with lower moisture content. The effectiveness of CP for reinforced concrete structures is strongly governed by the transport behavior of moisture and chloride ions within the concrete matrix. Chloride transport in concrete is closely coupled with moisture movement and occurs through a combination of diffusion, capillary absorption, and electromigration. The application of CP alters the electrochemical and transport processes within concrete. When a cathodic current is imposed, negatively charged chloride ions are repelled from the steel surface due to electromigration, while hydroxyl ions are generated at the cathode, increasing the local alkalinity. This process promotes repassivation of the reinforcing steel and reduces corrosion kinetics. The efficiency of these mechanisms, however, depends on the ability of the concrete pore solution to conduct current, which is directly influenced by moisture content and chloride concentration.

Fig. 8 presents the CP current density measured by sensors located in the submerged and atmospheric zones, along with the depolarization potential measured after 4 h of CP current interruption. As recommended by NACE SP0290, the effectiveness of cathodic protection for steel in concrete may be assessed by measuring the polarization

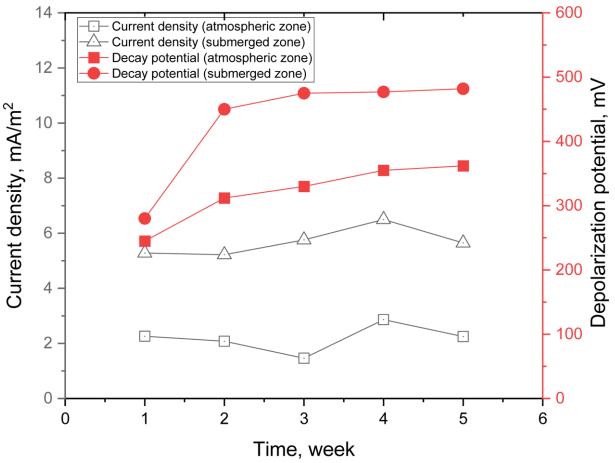

Fig. 8. Variation of cathodic protection current density measured from sensors located in the submerged and atmospheric zones, and depolarization potential after 4 hours of power off the cathodic protection current supply every weeks

decay after interruption of the CP current, where a depolarization of at least 100 mV within a period of up to 4 h is generally accepted as evidence of adequate corrosion protection. The depolarization represents the potential shift from the CP potential to the natural corrosion potential following disconnection of the ICCP system. Presuel-Moreno et al. reported that seawater and chloride absorption reduce concrete resistivity, thereby enabling effective current transfer from the anode to the reinforcement and sufficient polarization [14-16]. Consistent with this observation, the submerged zone in the present study exhibited larger depolarization values (430 ~ 490 mV) and higher CP current densities (5 ~ 6 mA/m^2), whereas the atmospheric zone showed relatively smaller depolarization values (310 ~ 350 mV) and lower CP current densities (2 ~ 3 mA/m^2). These differences are attributed to variations in moisture content with specimen height, which is consistent with the corrosion potential results. Nevertheless, in the present study, all monitored regions satisfied the 100 mV depolarization criterion and exceeded it by a substantial margin, confirming the effectiveness of the applied cathodic protection system.

4. Conclusions

Marine floating reinforced concrete offshore structures have been developed in parallel with the increasing demand for leisure activities in coastal and inland water

environments, where stable and abundant renewable energy sources are available. Considering the buoyant characteristics of floating structures, the mock-up specimen was divided into a submerged zone and an atmospheric zone to investigate the cathodic protection characteristics of an impressed current cathodic protection (ICCP) system.

In the initial state, the corrosion potentials of the atmospheric and submerged zones of the reinforced concrete specimen were measured as -308 mV/SSCE and -317 mV/SSCE, respectively. When the ICCP system was applied and the cathodic protection potential was controlled at -1000 mV/SSCE, a high initial cathodic protection current was supplied; however, it rapidly decreased and stabilized at less than 10 mA within a few minutes.

After interruption of the ICCP current supply, the depolarization potential measured after a 4 h rest period recovered to 310 ~ 350 mV in the atmospheric zone and 430 ~ 490 mV in the submerged zone. These results confirm that sufficient cathodic protection was achieved in all regions, satisfying the 100 mV depolarization criterion.

The concrete resistivity range of 0.9 ~ 1.5 kΩ under seawater exposure, as observed in this study, indicates that the reinforced concrete was subjected to a highly corrosive environment when evaluated solely based on resistivity. However, with the application of an ICCP system, such low-resistivity conditions are advantageous, as they facilitate efficient current transfer from the anode to the reinforcing steel, thereby enhancing corrosion protection performance.

In the future, eco-friendly floating reinforced concrete offshore structures capable of self-supplying energy through renewable sources such as wind power, solar power, and ocean thermal energy conversion are expected to be increasingly constructed in Korea, particularly in offshore regions where land-based power supply is not feasible. Accordingly, the application of impressed current cathodic protection systems to such structures is considered both practical and effective.

Acknowledgement

This work was supported by the Korea Maritime & Ocean University Research Fund in 2024.

References

1. Garrett Clark, Natthew Davis, Amit Kumar, Multi-measure pathways for achieving carbon-neutral cement production, *Sustainable Production and Consumption*, **57**, 355 (2025). Doi: https://doi.org/10.1016/j.spc.2025.05.025
2. Xiao-Guang Zhou, Chao Hou, Automated corrosion diagnosis of marine concrete-filled steel tubular structures using deep learning-based machine vision, *Automation in Construction*, **178**, 106403 (2025). Doi: https://doi.org/10.1016/j.autcon.2025.106403
3. H. Y. Chang, S. H. Hong, Y. S. Kim, Remote Monitoring and Controlling System for Cathodic Protection on Concrete Structure, *Corrosion Science and Technology*, **31**, 70 (2002). https://www.j-cst.org/opensource/pdfjs/web/pdf_viewer.htm?code=C00010100070
4. B. S. Jang, B. H. Oh, Experimental Study on Corrosion Rate in Concrete, *Corrosion Science and Technology*, **3**, 34 (2004). https://www.j-cst.org/opensource/pdfjs/web/pdf_viewer.htm?code=C00030100034
5. J. Kim, J. Lee, Estimation of The Global Warming Potential of Fluorinated Green House Gases, *Journal of Korean Society for Atmospheric Environment*, **30**, 387 (2014). Doi: https://doi.org/10.5572/KOSAE.2014.30.4.387
6. Mohammad Hasan Ramesht, Mohammad Ali Mehdizadeh Tavasani, A Case Study on Corrosion in Concrete Floating Docks in Qeshm Port, *Procedia Engineering*, **54**, 109 (2013) Doi: https://doi.org/10.1016/j.proeng.2013.03.010
7. Souvik Sen, Sourav Ganguly, Opportunities, barriers and issues with renewable energy development – A discussion, *Renewable and Sustainable Energy Reviews*, **69**, 1170 (2017) Doi: https://doi.org/10.1016/j.rser.2016.09.137
8. F. S. Al Masoodi and Falah K. Matloub, investigation the effect of ICCP and SACP on carbon steel corrosion in salt solution at different parameters, *Journal of Physics:Conference Series*, **1973**, 012031 (2021). Doi: https://doi.org/10.1088/1742-6596/1973/1/012031
9. K. C. Sohn, H. Y. Chang, Y. S. Kim, Lifetime of Insoluble Anode for Cathodic Protection on Concrete Construction, *Corrosion Science and Technology*, **4**, 56 (2005). https://www.j-cst.org/opensource/pdfjs/webpdf_viewer.htm?code=C00040200056
10. Guilherme Yuuki Koga, Blandine Albert, Ricardo Pereira Nogueira, Revisiting the ASTM C876 standard for corrosion of reinforcing steel: On the correlation between corrosion potential and polarization resistance during the

curing of different cement mortars, *Electrochemistry Communications*, **94**, 1 (2018). Doi: https://doi.org/10.1016/j.elecom.2018.07.017

11. W. Morris, A. Vico, M. Vazquez, S. R. de Sanchez, Corrosion of reinforcing steel evaluated by means of concrete resistivity measurements, *Corrosion Science*, **44**, 81 (2002). Doi: https://doi.org/10.1016/S0010-938X(01)00033-6
12. NACE International SP0290-2019, Impressed Current Cathodic Protection of Reinforcing Steel in Atmospherically Exposed Concrete Structures, Item No. 21043, ISBN 1-57590-103-X (2019). Doi: https://doi.org/10.5006/NACE_SP0290-2019
13. R. Pangrazzi, W. H. Hartt, R. Kessler, Cathodic Polarization and Protection of Simulated Prestraessed Concrete Pilings in Seawater, *Corrosion*, **50**, 186 (1994). Doi: https://doi.org/10.5006/1.3293510
14. F. J. Presuel-Moreno, S. C. Kranc, and A. A. Sagues, Cathodic Prevention Distribution in Partially Submerged Reinforced Concrete, *Corrosion Science*, **61**, 548 (2005). Doi: https://doi.org/10.5006/1.3278190
15. J. A. Jeong, K. H. Ko, M. S. Kim, D. H. Lee, A Study on the Effect of the ICCP System in Reinforced Concrete Specimens of Slab Type, *Corrosion Science and Technology*, **17**, 272 (2018) Doi: https://doi.org/10.14773/cst.2018.17.6.272
16. D. H. Lee, J. A. Jeong, Investigation of the Effective Range of Cathodic Protection for Concrete Pile Specimens Utilizing Zinc Mesh Anode, *Corrosion Science and Technology*, **23**, 195 (2024). Doi: https://doi.org/10.14773/cst.2024.23.3.195